

4-Pyridylanilinothiazoles That Selectively Target von Hippel–Lindau Deficient Renal Cell Carcinoma Cells by Inducing Autophagic Cell Death

Michael P. Hay,^{*,†} Sandra Turcotte,[‡] Jack U. Flanagan,[†] Muriel Bonnet,[†] Denise A. Chan,[‡] Patrick D. Sutphin,[‡] Phuong Nguyen,[‡] Amato J. Giaccia,[‡] and William A. Denny[†]

[†]Auckland Cancer Society Research Centre, Faculty of Medical and Health Sciences, The University of Auckland, Private Bag 92019, Auckland, New Zealand and [‡]Department of Radiation Oncology, Stanford University School of Medicine, Stanford, California 94305

Received October 1, 2009

Renal cell carcinomas (RCC) are refractory to standard therapy with advanced RCC having a poor prognosis; consequently treatment of advanced RCC represents an unmet clinical need. The von Hippel–Lindau (VHL) tumor suppressor gene is mutated or inactivated in a majority of RCCs. We recently identified a 4-pyridyl-2-anilinothiazole (PAT) with selective cytotoxicity against VHL-deficient renal cells mediated by induction of autophagy and increased acidification of autolysosomes. We report exploration of structure–activity relationships (SAR) around this PAT lead. Analogues with substituents on each of the three rings, and various linkers between rings, were synthesized and tested *in vitro* using paired RCC4 cell lines. A contour map describing the relative spatial contributions of different chemical features to potency illustrates a region, adjacent to the pyridyl ring, with potential for further development. Examples probing this domain validated this approach and may provide the opportunity to develop this novel chemotype as a targeted approach to the treatment of RCC.

Introduction

Renal cell carcinomas (RCCs⁶) represent a small but significant fraction of adult malignancies¹ and are refractory to standard chemotherapy and radiotherapy. Up to 45% of patients present locally advanced or metastatic disease,² and these patients have an extremely poor prognosis.³ The current standard of care, immunotherapy using interferon or interleukin-2, has modest success with responses in a small fraction of patients with metastatic RCC.⁴ Although recent antiangiogenic therapies such as sunitinib (Sutent) and sorafenib (Nexavar) have provided modest responses, it remains unclear which patients will have durable responses. This, combined with the observation of stable or increasing patient mortality,⁵ defines the treatment of advanced RCC as an unmet clinical need.

The von Hippel–Lindau (VHL) tumor suppressor gene is inactivated in ~75% of RCCs.^{6,7} This gene encodes for an E3 ubiquitin ligase that specifically regulates the protein stability of a family of transcription factors called hypoxia inducible factors (HIF).⁸ Loss of VHL results in constitutive expression of HIF leading to increased transcription of genes involved in metabolism, angiogenesis, invasion and metastasis, and proliferation leading to an aggressive phenotype.^{9–13} In addition to its role in HIF regulation, pVHL has been implicated in a variety of HIF-independent processes.^{14–17}

We recently developed a synthetic lethal^{18,19} screen to identify small molecules that are selectively cytotoxic to cells that have lost the VHL tumor suppressor gene.²⁰ Subsequently, we have screened several diverse chemical libraries and identified a number of “hits”. Hit compounds were validated in a growth inhibition assay, and the most promising compounds were further characterized by clonogenic survival assays. We demonstrated the pyridylanilinothiazole (PAT) chemotype (Figure 1) to be active in this context and found that compounds of this chemotype induced autophagy in both cell lines but led to cell death in a VHL-dependent fashion.²¹ The lead molecule, STF-62247 (**11**) (Table 1), reduced tumor growth *in vivo* in VHL-deficient RCC compared to genetically matched cells that express wild-type VHL.²¹

In this study, we have synthesized a range of analogues (**1–106**) with substituents on each ring of the PAT chemotype as well as modifications to the linker units between the three domains. We have examined their *in vitro* activity as VHL-selective cytotoxins using paired renal cell carcinoma cell lines: the VHL-null cell line RCC4 and the matched line RCC4-VHL, which has VHL function restored. These well characterized cell lines are isogenic with the exception of VHL status.⁸ The selectivity of the analogues was determined as the ratio (RCC4-VHL GI₅₀)/(RCC4 GI₅₀). We have examined the structure–activity relationships (SAR) for VHL-selective cytotoxicity. A quantitative analysis of these SAR was used to develop a common molecular alignment for VHL-selective members of the chemotype, and this alignment was used to predict cytotoxicity and assessed as a tool to guide further analogue synthesis. Initial attempts to use this tool to direct synthesis are reported.

*To whom correspondence should be addressed. Phone: 64-9-9236598. Fax: 64-9-3737502. E-mail: m.hay@auckland.ac.nz.

^aAbbreviations: RCC, renal cell carcinoma; VHL, von Hippel–Lindau; HIF, hypoxia-inducible factor; PAT, pyridylanilinothiazole; SAR, structure–activity relationship; CoMFA, comparative molecular field analysis; PLS, partial least-squares.

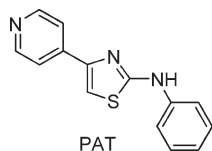
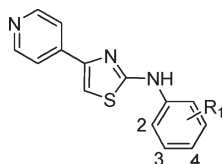


Figure 1

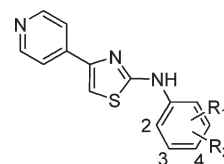
Table 1. GI₅₀ Values and Selectivity Ratios for Substituted 4-PATs

compd	R ₁	RCC4 GI ₅₀ , ^a μM	ratio ^b
1	H	7	> 10
2	2-OH	12.8	> 3.1
3	2-OMe	33.4	> 1.2
4	2-Me	> 40	nd ^c
5	2-Fl	14.3	> 2.8
6	2-Cl	27.6	> 1.4
7	2-CF ₃	> 40	nd ^c
8	2-NO ₂	> 40	nd ^c
9	3-OH	28.5	> 3
10	3-OMe	3	17
11	3-Me	2.1	19
12	3-Et	2.5	9.6
13	3-iPr	17	1.4
14	3-tBu	> 40	nd ^c
15	3-F	> 40	nd ^c
16	3-Cl	3	5
17	3-Br	12.4	> 3.2
18	3-CN	> 40	nd ^c
19	3-CF ₃	> 40	nd ^c
20	3-NO ₂	> 40	nd ^c
21	4-OH	5.3	8
22	4-OMe	14	3.6
23	4-OCH ₂ CH ₂ NMe ₂	60	1.3
24	4-Me	2.5	20
25	4-CH ₂ CH ₂ OH	5	16
26	4-CH ₂ CH ₂ NMe ₂	50	1.2
27	4-F	6	> 7
28	4-Cl	38	> 2
29	4-CN	> 40	nd ^c
30	4-CF ₃	> 40	nd ^c
31	4-NO ₂	> 40	nd ^c
32	4-NH ₂	nt ^d	nt ^d

^a Single determinations in triplicate. ^b Ratio = (RCC4-VHL GI₅₀)/(RCC4 GI₅₀). ^c nd, not determined because of low solubility. ^d nt, not tested.

Chemistry

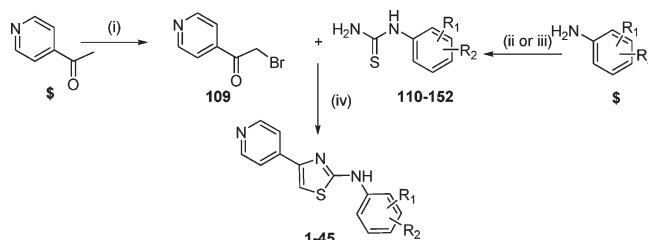
Synthesis. Initially, we synthesized a set of analogues (1–45) with substituents on the aniline ring (Tables 1 and 2). These analogues were conveniently prepared using the Hantzsch thiazole synthesis, condensing pyridylbromoketones with phenylthioureas (Scheme 1). 4-Pyridyl-2-bromoethanone **109** was readily prepared from 4-acetylpyridine using Br₂ in HBr/HOAc. Thioureas **110–152** were commercially available or were prepared from the corresponding aniline. Direct reaction of the appropriate aniline and NH₄SCN in acidic solution readily provides thioureas, albeit in low to moderate yields. For less accessible (or more

Table 2. GI₅₀ Values and Selectivity Ratios for Substituted 4-PATs

compd	R ₁	R ₂	RCC4 GI ₅₀ , ^a μM	ratio ^b
33	2-Fl	6-Fl	> 40	nd ^c
34	2-Me	6-Me	> 40	nd ^c
35	3-Me	4-Me	6.5	6.4
36	3-Me	5-Me	4.5	> 9
37	3-CH ₂ -CH ₂ -4		2.0	10
38	3-OH	4-Me	12	4.6
39	3-OH	4-OMe	nt ^d	nt ^d
40	3-Me	4-OH	70	2.3
41	3-OMe	4-OMe	24	1.9
42	3-OMe	5-OMe	> 40	nd ^c
43	3-OCH ₂ O-4		> 40	nd ^c
44	3-Cl	4-Cl	13.5	> 3
45	3,4,5-OMe ₃		> 40	nd ^c

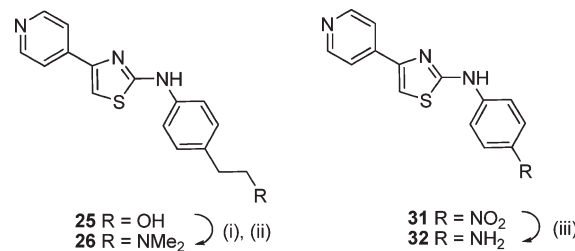
^a Single determinations in triplicate. ^b Ratio = (RCC4-VHL GI₅₀)/(RCC4 GI₅₀). ^c nd, not determined because of low solubility. ^d nt, not tested.

Scheme 1^a



^a Reagents: (i) Br₂, HOAc/HBr; (ii) NH₄SCN, aqueous HCl; (iii) PhCOCl, NH₄SCN, acetone, then aqueous NaOH; (iv) EtOH. \$ = commercially available.

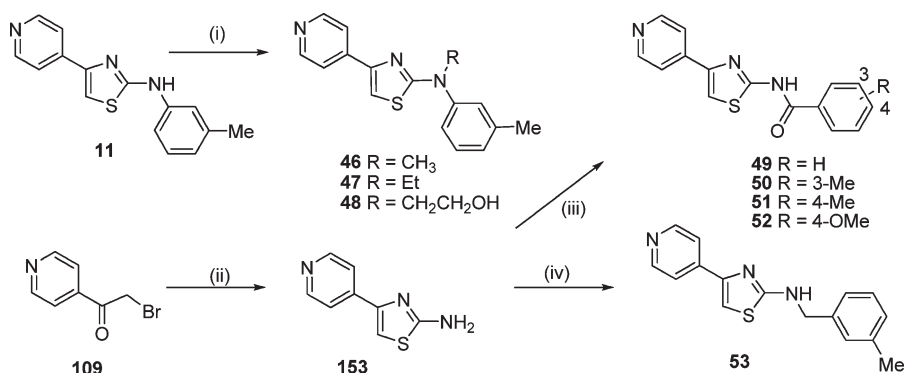
Scheme 2^a



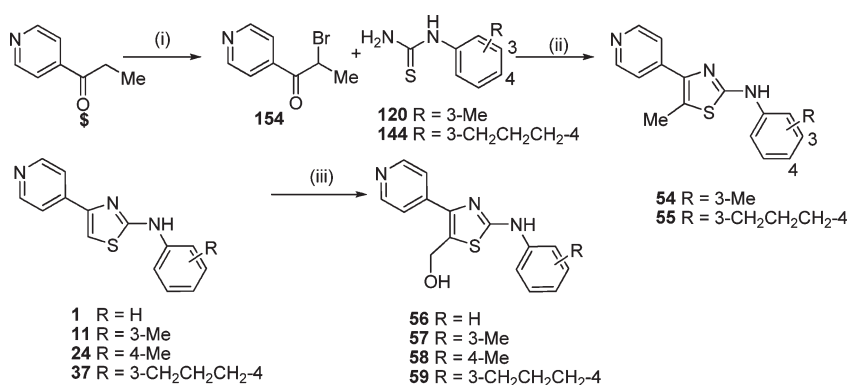
^a Reagents: (i) MsCl, *i*-Pr₂NEt, DCM; (ii) Me₂NH, DMF; (iii) H₂, Pd/C, EtOH.

expensive) anilines, reaction of benzoyl isocyanate and aniline to give corresponding benzoyl thioureas followed by hydrolysis provided higher yields.²² Elaboration of the primary alcohol **25** to the dimethylamine **26**, and reduction of the nitroaniline **31** to aminoaniline **32**, was accomplished using standard chemistries (Scheme 2).

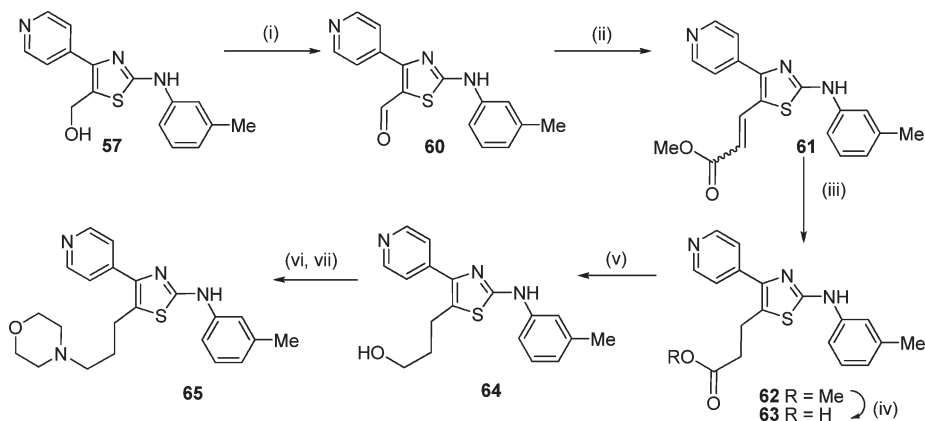
Modification of the linker between the thiazole and aniline rings was examined. Alkylation at the 2-amino position of **11**

Scheme 3^a

^a Reagents: (i) NaH, RI, DMF; (ii) NH₂C(SNH₂), EtOH; (iii) benzoic acid, (COCl)₂, DMF, DCM; (iv) 3-methylbenzaldehyde, THF; then NaBH₄, H₂O.

Scheme 4^a

^a Reagents: (i) Br₂, HOAc/HBr; (ii) EtOH; (iii) HCHO, Et₃N, THF. \$ = commercially available.

Scheme 5^a

^a Reagents: (i) MnO₂, benzene; (ii) Ph₃P=CHCO₂Me, DCM; (iii) H₂, Pd/C, EtOH, EtOAc; (iv) NaOH, EtOH; (v) LiAlH₄, THF; (vi) MsCl, *i*-Pr₂NEt, DCM; (vii) morpholine, DMF.

gave the 2-alkylaminothiazoles **46–48** (Scheme 3). Reaction of bromoketone **109** with thiourea gave the 2-aminothiazole **153**, which was reacted with a series of acid chlorides to give the amides **49–52**. Reductive amination of **153** with 3-methylbenzaldehyde gave the secondary amine **53**.

Bromination of 4-pyridylpropanone gave the bromide **154**, which was coupled with thioureas **120** and **144** to give 5-methylthiazoles **54** and **55**, respectively (Scheme 4). Formylation of pyridylthiazoles (**1**, **11**, **24**, and **37**) gave the corresponding 5-hydroxymethyl analogues **56–59**. Oxidation of hydroxymethylthiazole **57** gave aldehyde **60**, which

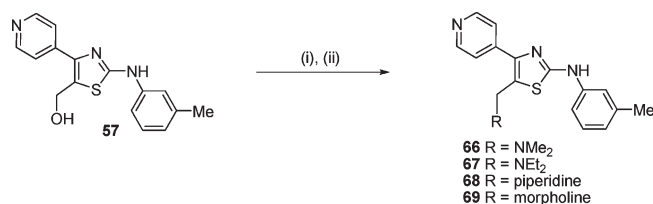
underwent Wittig reaction to give a mixture of *E* and *Z* isomers of the unsaturated ester **61** (Scheme 5). Reduction of **61** gave the ester **62**, which was hydrolyzed to the acid **63** and then reduced to the propanol **64**. Mesylation and reaction with morpholine gave the morpholide **65**. The hydroxymethylthiazole **57** was further elaborated to a series of solubilized thiazole analogues **66–69** (Scheme 6). Bromination of ethyl isonicotinoylacetate gave the bromoketoester **155** which was condensed with thioureas **120** and **144** to give 5-ethylesters **70** and **71**, respectively (Scheme 7). Hydrolysis of ester **70** and coupling with a variety of amines gave the amides **73–76**.

Isomeric 2- and 3-pyridyl analogues **77–82** were readily prepared by reaction of the bromides **156** and **157** with thioureas **110**, **120**, and **130** (Scheme 8). Modification of the linker between the pyridine and thiazole rings was examined. The bromides **160** and **163** could be conveniently prepared from the 2- and 3-pyridylethanones by an extension of a regioselective bromination/debromination strategy.²³ Conversion of 3- or 4-pyridineacetic acid to their Weinreb amides, **158** and **161**, and then to the corresponding methyl ketones, **159** and **162**, with subsequent bromination and condensation with thiourea **120** gave pyridylmethylthiazoles **83** and **84** with extended linker chains.

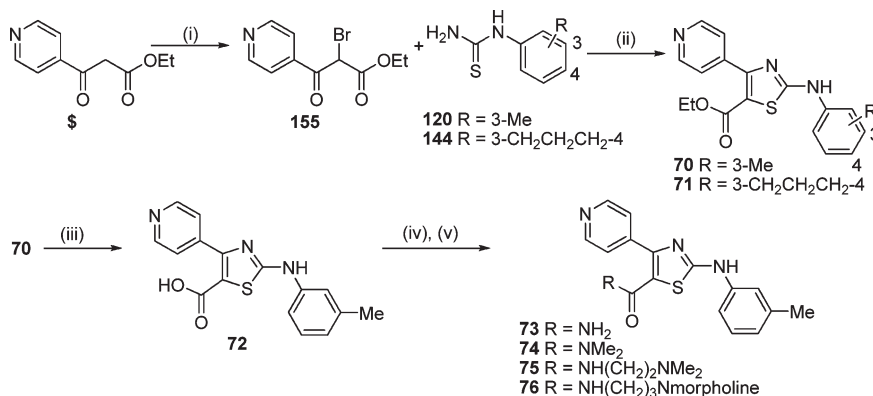
Finally, we sought to elaborate the pyridine ring to explore the SAR for this domain. Thus, reaction of amine **11** with MCPBA gave the *N*-oxide **85** (Scheme 9). In most instances preparation of the Weinreb amides of 4-pyridinecarboxylic acids and Grignard reaction with MeMgBr gave 4-ethanones,^{24,25} which were brominated and condensed with **120** to give the corresponding PATs (Schemes 9 and 10). The

2-methoxypyridine acid was converted to the acid chloride and treated with TMSCH₂N₂, and the intermediate diazo-ketone was treated with HBr to give the bromoketone **164** (Scheme 9). The 2-Me analogue **167** was obtained by reaction of 2-picoline *N*-oxide with Me₂SO₄ and KCN to give the nitrile **165**. Grignard reaction gave the ketone **166** which was brominated to give **167**. Elaboration of the 2-Br PAT **90** using Stille chemistry [Pd(PPh₃)₄, allyltributyltin] proved to be unsuccessful, but the application of Sonogashira chemistry was effective. Thus, reaction of bromide **90** with TMS-acetylene in the presence of PdCl₂(PPh₃)₂ and CuI, followed by removal of the TMS protecting group with TBAF, gave the 2-alkyne **92** in moderate yield. Reduction of the acetylene group gave the 2-ethyl analogue **93**. A similar sequence with propargyl alcohol gave the 2-substituted propynol **94** and the corresponding propanol **95**. A series of 3-substituted pyridines **96–100** were synthesized via Weinreb amide chemistry (Scheme 10). The 3-nitro PAT **100** was reduced to the 3-amino PAT **101** with subsequent acetylation giving acetamide **102**. Sonogashira chemistry was used to elaborate the 3-bromo PAT **99** to a series of 3-alkynyl and 3-alkyl PATs **103–106**.

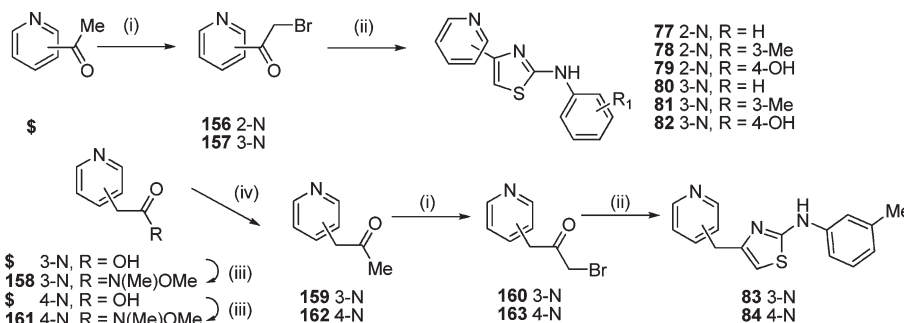
In preliminary experiments to explore modeling predictions, we synthesized two additional analogues. Sonogashira reaction of bromide **99** gave the methyl ether **107**, while Suzuki reaction of bromide **99** gave the phenyl ketone **108**.

Scheme 6^a

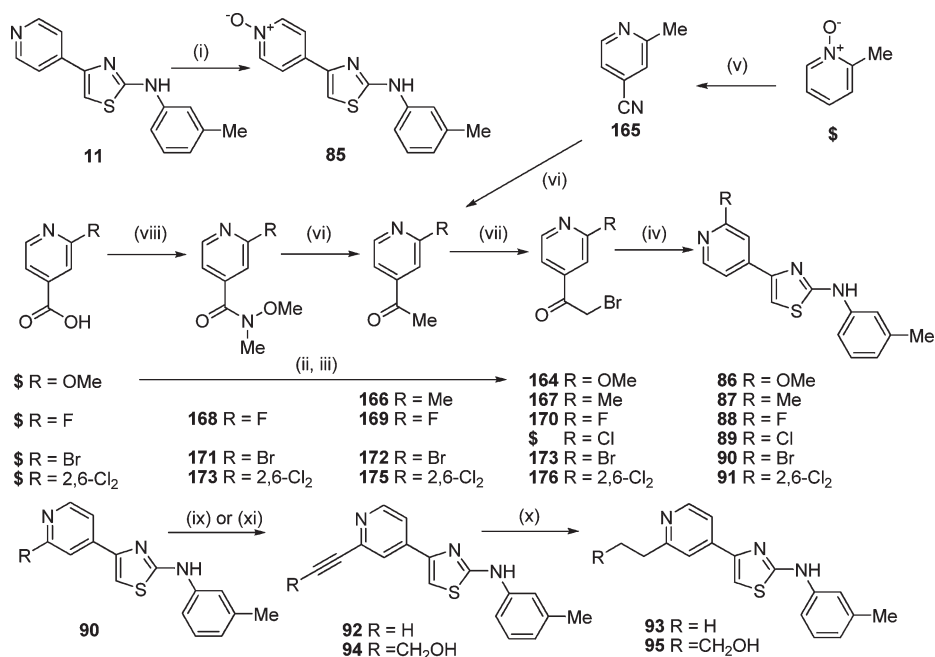
^a Reagents: (i) MsCl, *i*-Pr₂NEt, DCM; (ii) amine, DMF.

Scheme 7^a

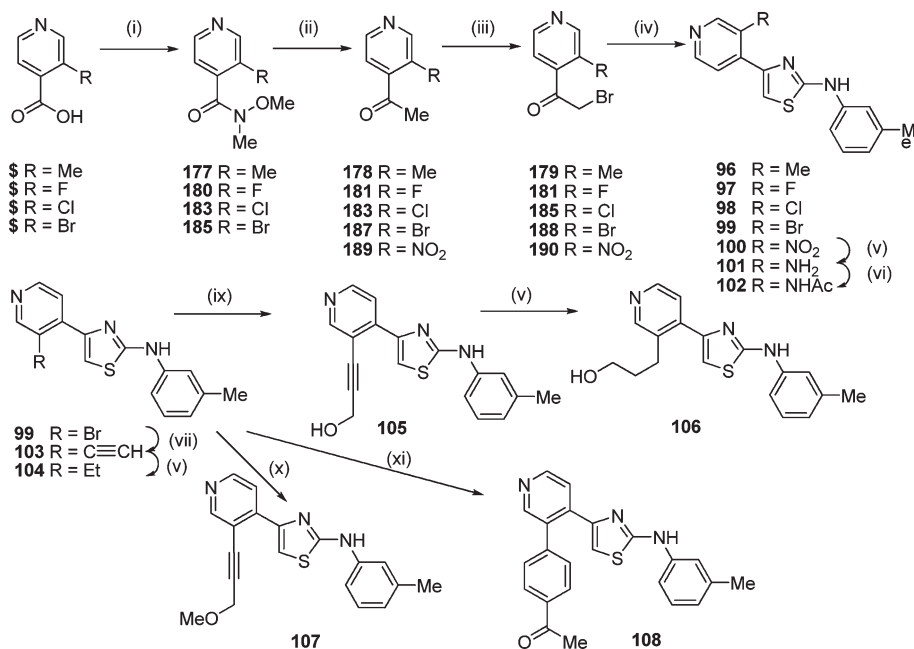
^a Reagents: (i) Br₂, CHCl₃; (ii) EtOH; (iii) NaOH, EtOH; (iv) (COCl)₂, DMF, DCM; (v) amine, DCM. \$ = commercially available.

Scheme 8^a

^a Reagents: (i) Br₂, HOAc/HBr; (ii) arylthiourea, EtOH; (iii) MeNHOMe, EDCl, HOBT, Et₃N, DCM; (iv) MeMgBr, THF. \$ = commercially available.

Scheme 9^a

^a Reagents: (i) MCPBA, DCM; (ii) (COCl)₂, DMF, DCM; (iii) TMSCH₂N₂, THF, then HBr; (iv) arylthiourea, EtOH; (v) Me₂SO₄, then KCN, aq EtOH; (vi) MeMgBr, THF; (vii) Br₂, HOAc/HBr; (viii) Me(OMe)NH·HCl, EDCI, HOBT, Et₃N, DCM; (ix) PdCl₂(PPh₃)₂, CuI, TMSC≡CH, Et₃N, DMF, then TBAF; (x) H₂, Pd/C, EtOH; (xi) PdCl₂(PPh₃)₂, CuI, HC≡CCH₂OH, Et₃N, DMF. \$ = commercially available.

Scheme 10^a

^a Reagents: (i) Me(OMe)NH·HCl, EDCI, HOBT, Et₃N, DCM; (ii) MeMgBr, THF; (iii) Br₂, HOAc/HBr; (iv) 3-methylphenylthiourea **118**, EtOH; (v) H₂, Pd/C, EtOH; (vi) Ac₂O, dioxane; (vii) PdCl₂(PPh₃)₂, CuI, TMSC≡CH, Et₃N, DMF, then TBAF; (ix) PdCl₂(PPh₃)₂, CuI, HC≡CCH₂OH, Et₃N, DMF; (x) PdCl₂(PPh₃)₂, CuI, HC≡CCH₂OMe, Et₃N, DMF; (xi) PdCl₂dppf, K₂CO₃, CH₃COPh(OH)₂, toluene, EtOH, H₂O, DMF. \$ = commercially available.

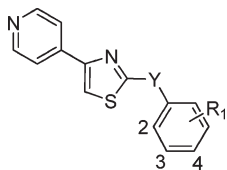
with default settings. The mmff94s force field was used for both construction and torsion driving, while the rms torsion driving parameter was set at 0.6. All other structures were generated from this conformation using the SKETCHER module in SYBYL8.0 (Tripos) and minimized using MAX-MIN2, with the Tripos force field and Gasteiger–Huckel charges. Minimization was performed using 1000 steps of step

descents followed by conjugate gradients until convergence at the 0.05 kcal/(mol·Å) level. A distance dependent dielectric function was used with a dielectric constant of 80. Where the compound could have more than one substitution pattern, all conformers were constructed. Molecules were superimposed on the basis of overlap of molecular volume using the ROCS alignment package (Openeyes) at default settings.

3D-QSAR Analysis. A comparative molecular field analysis (CoMFA)²⁶ 3D-QSAR method was used to determine a relationship between the compounds tested and in vitro cytotoxicity. Briefly, CoMFA was performed using a cubic lattice extending 4 Å around the aligned molecules with a point spacing of 2 Å. A distance dependent dielectric along with cutoffs of 30 kcal/mol and smooth transition were used for both steric and electrostatic energy calculations. A C.3 atom with charge +1 was used as the probe. The partial least-

squares (PLS) regression analysis was performed using the QSAR module, with the optimum number of components extracted from the standard error of predictions as determined using the SAMPLS protocol with leave-one-out cross-validation. The optimum number of components was used in the conventional nonvalidated PLS analysis. Only compounds that had both GI₅₀ and cytotoxicity ratios and substitutions up to one rotatable bond were used (41 compounds; see Supporting Information for set).

Table 3. GI₅₀ Values and Selectivity Ratios for Linkers



compd	R ₁	Y	RCC4 GI ₅₀ , ^a μM	ratio ^b
46	3-Me	NMe	28	0.6
47	3-Me	NEt	40	0.6
48	3-Me	NCH ₂ CH ₂ OH	> 40	nd ^c
49	H	NHCO	> 40	nd ^c
50	3-Me	NHCO	> 40	nd ^c
51	4-Me	NHCO	> 40	nd ^c
52	4-OMe	NHCO	> 40	nd ^c
53	3-Me	NHCH ₂	> 40	nd ^c

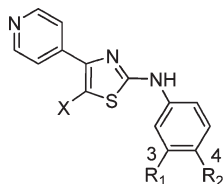
^aSingle determinations in triplicate. ^bRatio = (RCC4-VHL GI₅₀)/(RCC4 GI₅₀). ^cnd, not determined because of low solubility.

Biological Assays. Growth inhibition was determined by GI₅₀ assays, using a 4-day drug exposure of RCC4 and RCC4/VHL cells in 96-well plates as described previously.²¹ The selectivity ratio was calculated as the intraexperiment ratio RCC4-VHL/RCC4 (Tables 1–5). Selected compounds (**11**, **37**, **98**, and **105**) were tested in a clonogenic survival assay to assess their ability to kill RCC4 and RCC4/VHL cells in vitro. Three hundred cells were plated in 60 mm dishes and allowed to attach overnight. The next day, cells were treated with different concentrations of drug and colonies were stained 10 days later. These compounds were also examined for their ability to induce formation of intracytoplasmic vacuoles; thus, cells were incubated with drug (5 μM) for 24 h before phase contrast images were taken.

Results and Discussion

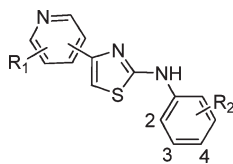
We have prepared a set of PAT analogues (**1–106**) designed to explore the SAR for each of the domains of the chemotype.

Table 4. GI₅₀ Values and Selectivity Ratios for Thiazole Substituents



compd	R ₁	R ₂	X	RCC4 GI ₅₀ , ^a μM	ratio ^b
54	Me	H	Me	10	> 4
55	3-CH ₂ CH ₂ CH ₂ -4	H	Me	12	1.5
56	H	H	CH ₂ OH	30	> 1.3
57	Me	H	CH ₂ OH	7	2.4
58	H	4-Me	CH ₂ OH	14	1.2
59	CH ₂ CH ₂ CH ₂	H	CH ₂ OH	6.8	1.4
60	Me	H	CHO	15	nd ^c
61	Me	H	CH=CHCO ₂ Me	2.5	2.8
62	Me	H	CH ₂ CH ₂ CO ₂ Me	> 40	nd ^c
63	Me	H	CH ₂ CH ₂ CO ₂ H	nt ^d	nt ^d
64	Me	H	CH ₂ CH ₂ CH ₂ OH	3.6	3.7
65	Me	H	CH ₂ HC(CH ₂) ₂ Nmorph	5.8	1.6
66	Me	H	CH ₂ NMe ₂	16	2.3
67	Me	H	CH ₂ NEt ₂	13	1.4
68	Me	H	CH ₂ N-piperidine	13	1.9
69	Me	H	CH ₂ N-morpholine	2.5	4.8
70	Me	H	CO ₂ Et	> 40	nd ^c
71	CH ₂ CH ₂ CH ₂	H	CO ₂ Et	> 40	nd ^c
72	Me	H	CO ₂ H	nt ^d	nt ^d
73	Me	H	CONH ₂	19.2	> 2
74	Me	H	CONMe ₂	16	> 2.5
75	Me	H	CONHCH ₂ CH ₂ NMe ₂	> 40	nd ^c
76	Me	H	CONHCH ₂ CH ₂ CH ₂ N-morph	> 40	nd ^c

^aSingle determinations in triplicate. ^bRatio = (RCC4-VHL GI₅₀)/(RCC4 GI₅₀). ^cnd, not determined because of low solubility. ^dnt, not tested.

Table 5. GI₅₀ Values and Selectivity Ratios for A Ring Substituents

compd	ring	R ₁	R ₂	RCC4 GI ₅₀ , ^a μM	ratio ^b
77	2-pyridyl	H	H	35.1	0.9
78	2-pyridyl	H	3-Me	37	0.9
79	2-pyridyl	H	4-OH	36	0.7
80	3-pyridyl	H	H	> 40	nd ^c
81	3-pyridyl	H	3-Me	> 40	nd ^c
82	3-pyridyl	H	4-OH	> 40	nd ^c
83	3-pyridyl-CH ₂	H	3-Me	> 40	nd ^c
84	4-pyridyl-CH ₂	H	3-Me	20.3	24.4
85	4-pyridyl- <i>N</i> -oxide	H	3-Me	> 40	nd ^c
86	4-pyridyl	2-OMe	3-Me	28.7	1.2
87	4-pyridyl	2-Me	3-Me	> 40	nd ^c
88	4-pyridyl	2-F	3-Me	4.5	> 8.9
89	4-pyridyl	2-Cl	3-Me	2.2	3.8
90	4-pyridyl	2-Br	3-Me	2.0	4.3
91	4-pyridyl	2,6-Cl ₂	3-Me	15	2.3
92	4-pyridyl	2-C≡CH	3-Me	17.8	> 2.2
93	4-pyridyl	2-Et	3-Me	6.4	> 6.3
94	4-pyridyl	2-C≡C-CH ₂ OH	3-Me	9.3	1.6
95	4-pyridyl	2-CH ₂ CH ₂ CH ₂ OH	3-Me	5.2	> 7.7
96	4-pyridyl	3-Me	3-Me	5.2	> 7.7
97	4-pyridyl	3-F	3-Me	2	> 20
98	4-pyridyl	3-Cl	3-Me	2.9	> 13.8
99	4-pyridyl	3-Br	3-Me	3.9	> 10
100	4-pyridyl	3-NO ₂	3-Me	8.2	4.1
101	4-pyridyl	3-NH ₂	3-Me	> 40	nd ^c
102	4-pyridyl	3-NHAc	3-Me	33.3	1.0
103	4-pyridyl	3-C≡CH	3-Me	1.35	4.4
104	4-pyridyl	3-Et	3-Me	6.2	2.8
105	4-pyridyl	3-C≡C-CH ₂ OH	3-Me	0.24	11.9
106	4-pyridyl	3-CH ₂ CH ₂ CH ₂ OH	3-Me	6.8	> 5.9
107	4-pyridyl	3-C≡C-CH ₂ OMe	3-Me	0.62	45
108	4-pyridyl	3-Ph-4-Ac	3-Me	3.9	9

^aSingle determinations in triplicate. ^bRatio = (RCC4-VHL GI₅₀)/(RCC4 GI₅₀). ^cnd, not determined because of low solubility.

Thus, a range of substituents on each of the aniline, thiazole, and pyridyl rings were synthesized, as well as analogues with modified linkers between the three rings. The ability of these analogues to inhibit cell growth in a VHL-dependent manner was investigated by determining the GI₅₀ values against a pair of renal cell carcinoma cell lines: the VHL-null cell line RCC4 and the matched line RCC4-VHL, which has VHL function restored. The selectivity of the analogues was determined as the ratio (RCC4-VHL GI₅₀)/(RCC4 GI₅₀). In many instances poor aqueous solubility prevented the determination of a GI₅₀ value against the RCC4-VHL cell line, leading to a greater value being expressed for the selectivity ratio. In the instances where inequalities were obtained for both cell lines the ratio was not determined.

The parent compound **1** was modestly potent with a GI₅₀ of 7 μM and selectivity for the VHL-negative RCC4 cell line of > 10-fold (Table 1). Addition of substituents to the 2-position of the aniline ring (**2–8**) was associated with a loss of potency and selectivity. Compounds with small, lipophilic substituents at the 3-position, such as the initial lead **11** with a 3-Me substituent, were active against the RCC4 cell line with low micromolar cytotoxicity and 10- to 20-fold selectivity. Increasing steric bulk in the 3-position (e.g., **12–14**) was

associated with a loss of potency and selectivity for RCC4. Polar substituents (e.g., **18–20**) resulted in inactive compounds. A similar theme was observed at the 4-position, where compounds with small lipophilic substituents such as 4-Me **24** and 4-F **27** had low micromolar potency, but increasing polarity at this position was associated with a loss of activity (e.g., **29–31**). Although an extended neutral side chain was tolerated in compound **25**, more polar analogues with basic amine side chains (**23, 26**) were less potent and not selective.

The SAR for multiply substituted anilines (**33–45**) mirrored that seen for single substituents (Table 2). 2, 6-Disubstitution was not tolerated, whereas dialkyl substituted compounds spanning the 3-, 4-, and 5-positions (**35–37**) had potencies similar to those of their monosubstituted counterparts but displayed lower selectivity. More polar combinations (**38–45**) resulted in diminished cytotoxic potency and a loss of selectivity.

Replacement of the aniline NH with an *N*-alkyl substituent (**46–48**) or conversion to an amide (**49–52**) or benzylamine (**53**) consistently abolished activity, suggesting a key binding interaction for the aniline NH (Table 3).

We next focused on substituents at the 5-position of the thiazole ring (Table 4). Although small alkyl substituents

(54–59) gave compounds with only slightly reduced cytotoxic potency, they suffered a complete loss of selectivity. Longer chain alkyl substituents with terminal polar groups (61–69) generally allowed retention of cytotoxic potency but resulted in low selectivity, suggesting off-target activity. Analogues with more polar ester or amide substituents (71, 73–76) were generally neither potent nor selective. Thus, substitution on the thiazole ring was not a fruitful endeavor.

Regioselectivity in the pyridine ring was explored with a series of 2- and 3-pyridyl analogues (77–82) (Table 5). These were all inactive as were 3- and 4-pyridyl analogues (83, 84) with a methylene spacer to the thiazole ring. Masking the 4-pyridyl moiety as the *N*-oxide (85) also ablated activity. Collectively, these data point to a key binding interaction for the 4-pyridyl moiety. Halide substituents at the 2-position of the pyridyl ring (88–91) gave potent analogues with low selectivity. Although the 2-methyl analogue 86 was inactive, higher analogues (93, 95) were potent and selective compounds. Incorporation of the acetylene unit (e.g., 92 and 94, respectively) resulted in compounds with lower potency and a loss of selectivity. The 3-halo substituted analogues (97–99) were potent and selective analogues, whereas more polar substituents (100–102) resulted in lower potency and a loss of selectivity. The 3-alkyl substitutions (96, 104, and 106) generated good potency and modest selectivity, and interestingly, the inclusion of an acetylene unit (103, 105) resulted in a clear increase in cytotoxic potency and selectivity.

3D-QSAR Model for Cell Cytotoxicity for the PAT Series.

Collectively, the SAR data provided inferences for further analogue development, but in the absence of information on the molecular target of the chemotype we sought to generate a more complete description of a possible bioactive conformation for the PAT chemotype by using CoMFA to assess the relationship between structure and differential cell killing ability using VHL selectivity.

Alignments that reflected the conformer possibilities for the substitutions present in the set of compounds used for

model development were tested. The data for the best model are presented in Table 6, and the putative bioactive conformation is shown in Figure 2 along with steric (Figure 2a) and electrostatic (Figure 2b) field contours. Although the data are limited in the GI₅₀ range they cover, and the low q^2 value indicates that the predictive value of this model is also limited, the data do provide some support for a relationship between this conformation of the PAT core and cytotoxicity and indicate that steric fields account for 65.6% of the variation in the data while electrostatic fields explain 34.4%.

Figure 2 shows that within the model development compound set, the contouring around the aniline ring is more complex than around the pyridine ring. A large blue contour around the 3-position of the aniline ring indicates that electrostatic effect around this site is favored while it is disfavored around the 4- and 5-positions. Only a region close to the 5-position of this ring reported a positive effect on GI₅₀ for steric bulk, while additional steric bulk around the 4-position is likely to have a negative effect. Compounds 23, 25, and 26 were not included in the QSAR analysis because of their flexibility; however, they probe this region with both steric bulk and electrostatic properties. The GI₅₀ values for the basic compounds increase, a result in part consistent with the disfavored electrostatic contour around this site; by contrast the smaller alkylhydroxyl side chain is accepted at this position with only a modest loss of activity, also supporting the yellow steric contour. Strikingly, the contour maps report the positive effect of steric bulk at the 3-position of the pyridine ring, while electrostatic effects around this region are likely to have a negative effect on GI₅₀.

Maintaining or increasing the selective cytotoxicity for RCC4 is important to the development of this series of compounds; thus, we overlaid those compounds with ratios of 10 or more (including 12, ratio 9.6) (Figure 2). Features common to compounds with high selectivity include the positive steric contour, green volume, at the pyridine ring 3-position while avoiding interaction with an adjacent disfavored electrostatic red region. In addition, selective compounds also had increased steric bulk around the 4- and 5-positions of the aniline ring while avoiding an interaction with the disfavored electrostatic region at the aniline 3- and 4-positions. Substituents on the pyridine ring provide the greatest potential for the definition of a new ligand domain.

We then tested the ability of the alignment to guide synthesis by exploring the steric pocket adjacent to the 3-position of the pyridyl ring. Two simple analogues of the existing series were prepared. Thus, synthesis of the

Table 6. Statistical Analysis of the QSAR Model

SAMPLS statistics	
LOO cross-validated q^2 (CV correlation coefficient)	0.344
<i>N</i> (no. of components)	3
SEP (standard error of prediction)	0.434
non-cross-validated r^2 (correlation coefficient)	0.825
SEE (standard error of estimate)	0.225
<i>F</i> (<i>F</i> ratio)	57.991
steric	0.656
electrostatic	0.344

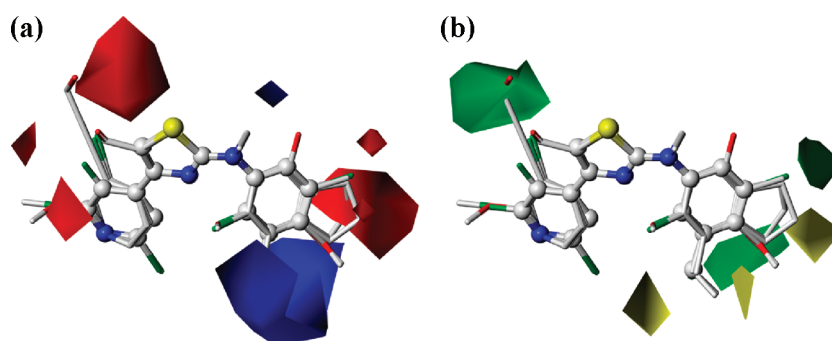
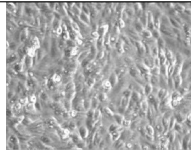
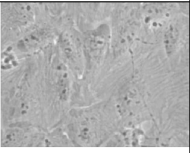
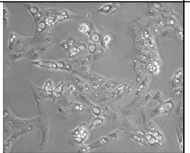
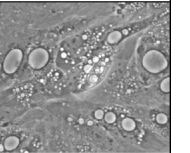
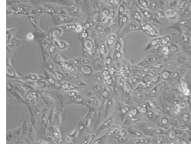
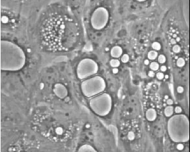
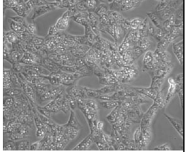
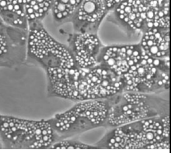
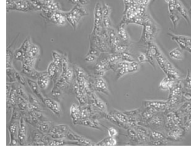
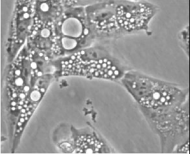
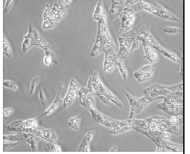
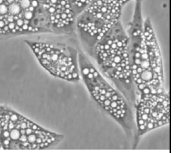


Figure 2. (a) 3D-QSAR conformer model relating PAT conformation to cytotoxicity. Electrostatic fields are contoured at 80% favored (blue) and 20% disfavored (red). (b) Steric fields are contoured at 80% favored (green) and 20% disfavored (yellow).

Table 7. Induction of Autophagy by PATs in RCC4 Cells

no	RCC4 -10X	RCC4 -40X	no	RCC4 -10X	RCC4 -40X
Control			98		
11			105		
37			107		

3-propargyl methyl ether **107** was achieved using a Sonogashira reaction with bromide **99** (Scheme 10). Similarly, Suzuki coupling of bromide **99** with 4-acetylphenylboronic acid gave the ketone **108**. The ether **107** retained VHL cytotoxic potency [$GI_{50(RCC4)} = 0.62 \mu\text{M}$] and was more selective (45-fold) when compared to the propargyl alcohol **105** (11-fold), confirming the potential use of the steric pocket to access improved PAT analogues. The use of a phenyl ring to probe the steric space was less successful, with **108** displaying low micromolar potency [$GI_{50(RCC4)} = 3.9 \mu\text{M}$] and modest selectivity (9-fold). The presence of this steric pocket may be useful when designing affinity chromatography reagents suitable for protein purification and identification studies.

We evaluated several of the more active compounds from the SAR set to confirm that their mechanism of action was the same as the initial lead **11**. Compounds **37**, **98**, and **105** were tested for their ability to suppress clonogenic survival and were shown to selectively kill RCC4 cells compared to RCC4/VHL (see Supporting Information for survival curves). Compounds **37**, **98**, **105**, and **107** were also examined for their ability to induce autophagy (Table 7). Treatment with the compounds ($5 \mu\text{M}$) for 24 h initiates the formation of intracytoplasmic vesicles in a similar manner to **11**, which in combination with the clonogenic data confirms the mode of action for these analogues as VHL-selective induction of autophagy resulting in cell death.

Conclusions

We have synthesized an exploratory SAR compound set to investigate the chemical space around the PAT chemotype. Empirical observation identified several key features necessary for selective cytotoxicity against VHL-negative renal carcinoma cells. The aniline-NH and the 4-pyridyl-N are likely to be involved in hydrogen bonding to the as yet undetermined molecular target, while an unsubstituted thiazole is required for VHL selectivity. The activities of compounds with small lipophilic substituents at the 3- and 4-positions of the aniline ring are suggestive of the presence of a lipophilic pocket in the molecular target. A subset of VHL-selective compounds was used to create a molecular alignment

to further explore the chemotype and develop a predictive model. CoMFA analysis suggested the alignment had low predictive power; however, the alignment did consistently interpret all the data. The alignment model also suggested the presence of a steric pocket adjacent to the 3-position of the pyridine ring that might provide a new domain for analogue development. Preliminary efforts to explore this pocket were successful with two analogues displaying increased VHL-selective cytotoxicity. The activity of these additional analogues demonstrates the potential of the alignment to identify new domains to explore in the search for more potent and selective VHL-dependent cytotoxins. Further studies are currently underway to utilize the QSAR around this chemotype to improve potency and selectivity, as well as to develop tools to explore the novel mechanism of action of the class. This will enable further development of this novel targeted approach to the treatment of renal cell carcinoma.

Experimental Section

Chemistry. General experimental details are described in the Supporting Information. All final products were analyzed by reverse-phase HPLC (Altima C18 $5 \mu\text{m}$ column, $150 \text{ mm} \times 3.2 \text{ mm}$; Alltech Associated, Inc., Deerfield, IL) using an Agilent HP1100 equipped with a diode-array detector. Mobile phases were gradients of 80% acetonitrile/20% H_2O (v/v) in 45 mM ammonium formate at pH 3.5 and 0.5 mL/min. Purity was determined by monitoring at $330 \pm 50 \text{ nm}$ and was $>95\%$ in all cases.

Example of Synthetic Methods. See Supporting Information for full experimental details.

Method A. Preparation of Pyridyl-2-bromoethanones. Br_2 (80 mmol) was added dropwise to a stirred solution of acetylpyridine (80 mmol) in 30% HBr/HOAc (100 mL) at 15°C . The mixture was stirred at 40°C for 1 h and then at 75°C for 1 h. The mixture was cooled to 20°C , diluted with Et_2O (400 mL), and stirred for 30 min. The precipitate was filtered, washed with Et_2O (25 mL), and dried under vacuum to give the bromoethanone as the hydrobromide salt.

Method B. Preparation of Thioureas. NH_4SCN (50 mmol) was added to a stirred solution of *m*-toluidine (50 mmol) in 1 M HCl (50 mL) at 100°C and the solution stirred at 100°C for 16 h. The solution was diluted with water (60 mL) and stood at 5°C for 2 h. The precipitate was filtered, washed with water (5 mL),

washed with ether (5 mL), and dried. The precipitate was purified by column chromatography, eluting with an appropriate blend (30–100%) of EtOAc/petroleum ether, to give the thiourea.

Method C. Alternative Preparation of Thioureas. Benzoyl chloride (65 mmol) was added dropwise to a solution of NH_4SCN (69 mmol) in dry acetone (50 mL). The mixture was stirred at reflux temperature for 15 min. The heating was removed, and *m*-toluidine (46 mmol) was added dropwise keeping the solution at reflux. The mixture was stirred at reflux temperature for a further 30 min, cooled to 20 °C, and poured onto ice. The mixture was stirred for 30 min, and then the precipitate was filtered and washed with water (15 mL) and dried. The solid was added to a solution of NaOH (10% w/v, 100 mL) at 80 °C and stirred at 80 °C for 30 min, then cooled to 20 °C and poured onto ice/HCl (6 M, 50 mL). The pH of the mixture was adjusted to 10 with concentrated NH_3 solution and stirred for 30 min. The precipitate was filtered and washed with water (20 mL) and dried. The precipitate was purified by column chromatography, eluting with an appropriate blend (30–100%) of EtOAc/petroleum ether, to give the thiourea.

Method D. Preparation of Thiazoles. A mixture of bromoketone hydrobromide (3 mmol) and phenylthiourea (3 mmol) in EtOH (20 mL) was stirred at reflux temperature for 1 h. The mixture was cooled to 20 °C and diluted with water (50 mL), the pH adjusted to ~8 with aqueous NH_3 , and the mixture stirred at 20 °C for 2 h. The precipitate was filtered, washed with water (5 mL), and dried. The solid was purified by column chromatography, eluting with an appropriate blend (30–100%) of EtOAc/petroleum ether, to give the thiazole.

Method E. Preparation of Pyridylamides. Et_3N (6.0 mmol) was added to a stirred suspension of 4-pyridinylacetic acid (1.5 mmol), EDCI (1.7 mmol), HOBT· H_2O (1.7 mmol), and MeN-HOME·HCl (2.3 mmol) in dry DCM (50 mL), and the mixture was stirred at 20 °C for 16 h. The resulting solution was diluted with DCM (100 mL), washed with water (2 × 30 mL), washed with brine (30 mL), and dried, and the solvent was evaporated. The residue was purified by column chromatography, eluting with a gradient of an appropriate blend (0–10%) of MeOH/EtOAc, to give the amide.

Method F. Preparation of Pyridyl Ketones. A solution of MeMgBr (3 M in hexanes, 7.5 mmol) was added slowly to a stirred solution of amide (5 mmol) in dry THF (50 mL) at 0 °C, and the mixture was stirred at 0 °C for 8 h. The reaction mixture was quenched with saturated aqueous NH_4Cl solution (20 mL) and the mixture extracted with EtOAc (3 × 50 mL). The combined organic fraction was washed with water (40 mL), washed with brine (40 mL), and dried, and the solvent was evaporated. The residue was purified by column chromatography, eluting with 30% EtOAc/petroleum ether, to give ketone.

GI₅₀ Assays. GI₅₀ values for compounds were determined by XTT assay. For 2,3-bis[2-methoxy-4-nitro-5-sulfophenyl]-2H-tetrazolium-5-carboxanilide inner salt (XTT) assays, 5000 cells were plated in 96-well plates. The next day, vehicle or drug was added to each well and incubated for 4 days. The medium was aspirated, and phenol red-free medium with 0.3 mg/mL XTT (Sigma Chemical Co) in phenol red-free medium, 20% FCS, and 2.65 μg/mL *N*-methylidibenzopyrazine methyl sulfate was added. The cells were incubated at 37 °C for 1–2 h, and absorbance was read at 450 nm. GI₅₀ values for each compound were calculated using linear interpolation.

Clonogenic Assays. Three hundred cells were plated into 60 mm tissue culture dishes in DMEM. The next day, cells were treated with vehicle or drug and were further incubated for an additional 10 days. After 10 days, the medium was removed and colonies were fixed and stained in 95% ethanol and 0.1% crystal violet for 15 min. The stain was removed, and plates were washed in deionized water. Colonies were quantified. All conditions were measured in triplicate, and all experiments were performed in triplicate.

Acknowledgment. The authors thank Dr. Maruta Boyd and Sisira Kumara for technical assistance. This work was supported by the U.S. National Cancer Institute under Grant CA82566 (M.P.H., P.D.S.) and Grant CA123823 (D.A.C.), by Canadian Institutes of Health Research (S.T.), and by the Auckland Division of the Cancer Society of New Zealand (W.A.D.).

Supporting Information Available: Experimental details and characterization data for synthetic intermediates **109–190** and PATs **1–108**. This material is available free of charge via the Internet at <http://pubs.acs.org>.

References

- (1) Jemal, A.; Siegel, R.; Ward, E.; Hao, Y.; Xu, J.; Thun, M. J. Cancer statistics, 2009. *Ca—Cancer J. Clin.* **2009**, *59*, 225–249.
- (2) Chow, W. H.; Devesa, S. S.; Warren, J. L.; Fraumeni, J. F., Jr. Rising incidence of renal cell cancer in the United States. *JAMA, J. Am. Med. Assoc.* **1999**, *281*, 1628–1631.
- (3) Motzer, R. J.; Mazumdar, M.; Bacik, J.; Berg, W.; Amsterdam, A.; Ferrara, J. Survival and prognostic stratification of 670 patients with advanced renal cell carcinoma. *J. Clin. Oncol.* **1999**, *17*, 2530–2540.
- (4) Nelson, E. C.; Evans, C. P.; Lara, P. N., Jr. Renal cell carcinoma: current status and emerging therapies. *Cancer Treat. Rev.* **2007**, *33*, 299–313.
- (5) Murai, M.; Oya, M. Renal cell carcinoma: etiology, incidence and epidemiology. *Curr. Opin. Urol.* **2004**, *14*, 229–233.
- (6) Gnarr, J. R.; Tory, K.; Weng, Y.; Schmidt, L.; Wei, M. H.; Li, H.; Latif, F.; Liu, S.; Chen, F.; Duh, F.-M.; Lubensky, I.; Duan, D. R.; Florence, C.; Pozzatti, R.; Walther, M. M.; Bander, N. H.; Grossman, H. B.; Brauch, H.; Pomer, S.; Brooks, J. D.; Isaacs, W. B.; Lerman, M. I.; Zbar, B.; Linehan, W. M. Mutations of the VHL tumour suppressor gene in renal carcinoma. *Nat. Genet.* **1994**, *7*, 85–90.
- (7) Kim, W. Y.; Kaelin, W. G. Role of VHL gene mutation in human cancer. *J. Clin. Oncol.* **2004**, *22*, 4991–5004.
- (8) Maxwell, P. H.; Wiesener, M. S.; Chang, G. W.; Clifford, S. C.; Vaux, E. C.; Cockman, M. E.; Wykoff, C. C.; Pugh, C. W.; Maher, E. R.; Ratcliffe, P. J. The tumour suppressor protein VHL targets hypoxia-inducible factors for oxygen-dependent proteolysis. *Nature* **1999**, *399*, 271–275.
- (9) Gnarr, J. R.; Zhou, S.; Merrill, M. J.; Wagner, J. R.; Krumm, A.; Papavassiliou, E.; Oldfield, E. H.; Klausner, R. D.; Linehan, W. M. Post-transcriptional regulation of vascular endothelial growth factor mRNA by the product of the VHL tumor suppressor gene. *Proc. Natl. Acad. Sci. U.S.A.* **1996**, *93*, 10589–10594.
- (10) Iliopoulos, O.; Levy, A. P.; Jiang, C.; Kaelin, W. G., Jr.; Goldberg, M. A. Negative regulation of hypoxia-inducible genes by the von Hippel–Lindau protein. *Proc. Natl. Acad. Sci. U.S.A.* **1996**, *93*, 10595–10599.
- (11) Knebelmann, B.; Ananth, S.; Cohen, H. T.; Sukhatme, V. P. Transforming growth factor alpha is a target for the von Hippel–Lindau tumor suppressor. *Cancer Res.* **1998**, *58*, 226–231.
- (12) Staller, P.; Sulitkova, J.; Lisztwan, J.; Moch, H.; Oakeley, E. J.; Krek, W. Chemokine receptor CXCR4 downregulated by von Hippel–Lindau tumour suppressor pVHL. *Nature* **2003**, *425*, 307–311.
- (13) Erler, J. T.; Bennewith, K. L.; Nicolau, M.; Dornhofer, N.; Kong, C.; Le, Q. T.; Chi, J. T.; Jeffrey, S. S.; Giaccia, A. J. Lysyl oxidase is essential for hypoxia-induced metastasis. *Nature* **2006**, *440*, 1222–1226.
- (14) Ohh, M.; Yauch, R. L.; Lonergan, K. M.; Whaley, J. M.; Stemmer-Rachamimov, A. O.; Louis, D. N.; Gavin, B. J.; Kley, N.; Kaelin, W. G., Jr.; Iliopoulos, O. The von Hippel–Lindau tumor suppressor protein is required for proper assembly of an extracellular fibronectin matrix. *Mol. Cell* **1998**, *1*, 959–968.
- (15) Hergovich, A.; Lisztwan, J.; Barry, R.; Ballschmieter, P.; Krek, W. Regulation of microtubule stability by the von Hippel–Lindau tumour suppressor protein pVHL. *Nat. Cell Biol.* **2003**, *5*, 64–70.
- (16) Okuda, H.; Saitoh, K.; Hirai, S.; Iwai, K.; Takaki, Y.; Baba, M.; Minato, N.; Ohno, S.; Shuin, T. The von Hippel–Lindau tumor suppressor protein mediates ubiquitination of activated atypical protein kinase C. *J. Biol. Chem.* **2001**, *276*, 43611–43617.
- (17) Na, X.; Duan, H. O.; Messing, E. M.; Schoen, S. R.; Ryan, C. K.; di Sant’Agnese, P. A.; Golemis, E. A.; Wu, G. Identification of the RNA polymerase II subunit hSRP7 as a novel target of the von Hippel–Lindau protein. *EMBO J.* **2003**, *22*, 4249–4259.

- (18) Sutphin, P. D.; Chan, D. A.; Giaccia, A. J. Dead cells don't form tumors: HIF-dependent cytotoxins. *Cell Cycle* **2004**, *3*, 160–163.
- (19) Kaelin, W. G., Jr. The concept of synthetic lethality in the context of anticancer therapy. *Nat. Rev. Cancer* **2005**, *5*, 689–689.
- (20) Sutphin, P. D.; Chan, D. A.; Li, J. M.; Turcotte, S.; Krieg, A. J.; Giaccia, A. J. Targeting the loss of the von Hippel–Lindau tumor suppressor gene in renal cell carcinoma cells. *Cancer Res.* **2007**, *67*, 5896–5905.
- (21) Turcotte, S.; Sutphin, P. D.; Chan, D. A.; Hay, M. P.; Denny, W. A.; Giaccia, A. J. A novel molecule targeting VHL-deficient renal cell carcinoma that induces autophagic cell death. *Cancer Cell* **2008**, *14*, 90–102.
- (22) Rasmussen, C. R.; Villani, F. J., Jr.; Weaner, L. E.; Reynolds, B. E.; Hood, A. R.; Hecker, L. R.; Nortey, S. O.; Hanslin, A.; Costanzo, M. J.; Powell, E. T.; Molinari, A. J. Improved procedures for the preparation of cycloalkyl-, arylalkyl-, and arylthioureas. *Synthesis* **1988**, 456–459.
- (23) Choi, H. Y.; Chi, D. Y. Non-selective bromination-selective debromination strategy: selective bromination of unsymmetrical ketones on singly activated carbon against doubly activated carbon. *Org. Lett.* **2003**, *5*, 411–414.
- (24) Nahm, S.; Weinreb, S. M. *N*-Methoxy-*N*-methylamides as effective acylating agents. *Tetrahedron Lett.* **1981**, *39*, 3815–3818.
- (25) Singh, J.; Satamurthi, N.; Aidhen, I. S. The growing synthetic utility of Weinreb's amide. *J. Prakt. Chem.* **2000**, *342*, 340–347.
- (26) Cramer, R. D.; Patterson, D. E.; Bunce, J. D. Comparative molecular field analysis (CoMFA): effect of shape on binding of steroids to carrier proteins. *J. Am. Chem. Soc.* **1988**, *110*, 5959–5967.